IJMMM International Journal of Minerals, Metallurgy and Materials 矿物冶金与材料学报（英文版）

Particle aggregation and breakage kinetics in cemented paste backfill

Liuhua Yang, Hengwei Jia, Aixiang Wu, Huazhe Jiao, Xinming Chen, Yunpeng Kou, and Mengmeng Dong

Cite this article as:
Liuhua Yang, Hengwei Jia, Aixiang Wu, Huazhe Jiao, Xinming Chen, Yunpeng Kou, and Mengmeng Dong, Particle aggregation and breakage kinetics in cemented paste backfill, *Int. J. Miner. Metall. Mater.*, 31(2024), No. 9, pp. 1965-1974. https://doi.org/10.1007/s12613-023-2804-5

INTERNATIONAL JOURNAL OF
Minerals, Metallurgy and Materials

Volume 31, Number 9, September 2024
Page 1965

Research Article https://doi.org/10.1007/s12613-023-2804-5

Particle aggregation and breakage kinetics in cemented paste backfill

Liuhua Yang[1),✉], *Hengwei Jia*[1)], *Aixiang Wu*[2)], *Huazhe Jiao*[1)], *Xinming Chen*[1)], *Yunpeng Kou*[2)], *and Mengmeng Dong*[1)]

1) School of Civil and Engineering, Henan Polytechnic University, Jiaozuo 454000, China
2) School of Civil and Environmental Engineering, University of Science and Technology Beijing, Beijing 100083, China
(Received: 4 May 2023; revised: 14 November 2023; accepted: 4 December 2023)

Abstract: The macroscopic flow behavior and rheological properties of cemented paste backfill (CPB) are highly impacted by the inherent structure of the paste matrix. In this study, the effects of shear-induced forces and proportioning parameters on the microstructure of fresh CPB were studied. The size evolution and distribution of floc/agglomerate/particles of paste were monitored by focused beam reflection measuring (FBRM) technique, and the influencing factors of aggregation and breakage kinetics of CPB were discussed. The results indicate that influenced by both internal and external factors, the paste kinetics evolution covers the dynamic phase and the stable phase. Increasing the mass content or the cement–tailings ratio can accelerate aggregation kinetics, which is advantageous for the rise of average floc size. Besides, the admixture and high shear can improve breaking kinetics, which is beneficial to reduce the average floc size. The chord length resembles a normal distribution somewhat, with a peak value of approximate 20 μm. The particle disaggregation constant (k_2) is positively correlated with the agitation rate, and k_2 is five orders of magnitude greater than the particle aggregation constant (k_1). The kinetics model depicts the evolution law of particles over time quantitatively and provides a theoretical foundation for the micromechanics of complicated rheological behavior of paste.

Keywords: cemented paste backfill; particle kinetics; admixture; rheology

1. Introduction

With the advancing of carbon peaking and carbon neutrality goals, and the proposal of the concept that clear water and lush mountains mean gold and silver mountains, the utilization of tailings resources and comprehensive treatment to environment have been attached great importance [1].

However, many vacant lands still appear and tailings are left on the surface due to the extraction of resources, which not only has led to environmental pollution and geological disasters, but also posed a significant threat to mine safety production [2–3]. Against such background, cemented paste backfill (CPB) technology is considered as a crucial research field for underground metal mining [4]. CPB technology is the resource utilization of solid waste such as tailings and slag to produce a paste that does not exude water, delaminate, or segregate [5–6]. Unlike traditional viscoplastic fluids, pastes exhibit high solid content and multiscale characteristics, leading to the complexity of their rheological behavior. Pastes exhibit specific rheological features such as solid–liquid transitions and shear thinning, resembling the rheological behaviour of non-Newtonian suspensions. Furthermore, their rheological properties are influenced by factors such as content, shear, and additives. In the present, the pivotal role of rheology in CPB has gained widespread recognition along with rheological studies delving into various process aspects of CPB. The paste is used to backfill the goaf to achieve safe, environmentally friendly, and efficient ore mining.

Rheology of paste is the study of slurry flow and deformation law [7]. CPB in metal mines mainly consists of four key processes: the thickening of tailings, the mixing of multiscale aggregates, the pipeline transportation of paste, and the backfill and solidification of paste in underground stope. It is the rheology that provides a theoretical foundation for these four processes. For the past few years, paste rheology has received extensive attention and in-depth research at home and abroad, and a lot of work has been done in rheological concepts, rheological properties and their influencing factors [8]. Accordingly, key research results have been achieved. When a paste is sheared, the stable mesh structure between the particles reacts to the shear stress, which is primarily determined by the contact forces between the particles. Consequently, having a deep understanding of the particle contact forces in paste slurries is a crucial precondition for the study of the rheological behavior of pastes. The reason is that pastes are more difficult to achieve *in situ* fine structure evolution monitoring due to their high concentration [9], low light transmission, and complex composition. In recent years, the fine-scale mechanisms that create complicated rheological behaviors in pastes have been ignored, and the majority of in-

✉ Corresponding author: Liuhua Yang E-mail: yanglh2005@163.com

vestigations of paste kinetics have been limited to hypotheses and numerical simulations. It is indicated that it's difficult to confirm the established model using experimental parameters and investigating the microscopic process underlying the non-Newtonian rheological behavior of the paste [10–11]. The inability to apply theoretical results to the prediction and regulation of rheological behavior has hindered the breakthrough of paste manufacturing and conveying technology [12–13]. In recent years, fine structural observations of concentration suspensions have become possible with the rapid developments of new technologies such as computed tomography (CT), electron microscopy, and focused beam reflection measuring (FBRM) [14]. Among them, computed tomography and electron microscopy have the advantages of high resolution, while they also present the disadvantages of requiring sample preparation for experiments and lagging data, which makes it impossible to get real-time dynamic evolution parameters. However, in addition to high precision (0.5 μm) and wide field of vision, the FBRM approach does not require sample extraction or preparation before the experiment, ensuring the reliability and instantaneity of experimental results. Based on FBRM, Yim *et al.* [15] analyzed the characteristics of flocs with time under various shear rate conditions by measuring the changes of fine microstructure of fresh concrete in shear flow. This work is significant for analyzing the properties of floc fluctuation at different shear rates and understanding the time-varying effects of thixotropic fluids [16–17]. Ferron *et al.* [18–19] carried out monitoring of the fine-scale structural evolution of cement paste using FBRM, analyzed the effect of factors such as thickeners and cohesive minerals on particle dynamics [20], and proposed a particle dynamics model that fitted the characteristics of cement paste. In order to optimize production parameters, FBRM is also utilized to observe the evolution of the floc structure during flocculation and settlement [21]. The above investigations fully demonstrate the technical benefits and feasibility of the FBRM technology in the field of studying the particle dynamics of high concentration suspensions.

To sum up, the key to comprehending the rheological behavior of highly concentrated, multi-scale particle suspensions is to investigate the expression of inter-particle forces. Through FBRM experiments performed on a copper ore tailing paste [22] to determine the fine-scale structure's particle number and chord length distribution features, the analysis of the tests demonstrates that the inter-particle forces are related to the degree of flocculation of the slurry, which is directly presented as a change in the particle aggregate size. Thus, this article proposes a kinetic particle model based on the Smoluchowski theory [23] and analyzes experimental data. In conjunction with inter-particle interactions, the number of particles and chord length distribution are used to systematically illustrate the law of paste slurry when it is influenced by content, cement–sand ratio, admixtures, and shear action. Through the analysis of the factors influencing the kinetic evolution of paste particles, the study reveals the kinetic mechanism of fine structure evolution, thus providing a theoretical basis for the paste preparation and performance regulation.

2. Experimental

2.1. Experiment materials

Tailings from a copper mine with a specific gravity of 2.72 were utilized in the research. The particle size distribution was determined by a laser particle size analyzer, and the results are shown in Fig. 1. From these, we can see that the particle sizes less than 20 and 74 μm were 54% and 87%, respectively, which can be classified as fine tailing sand according to the industry standards [24]. As shown in Table 1, the chemical composition is analyzed by X-ray fluorescence spectroscopy (XRF). The main components of tailings are SiO_2, CaO, MgO, Al_2O_3, etc.

The cementitious material is made of ordinary Portland

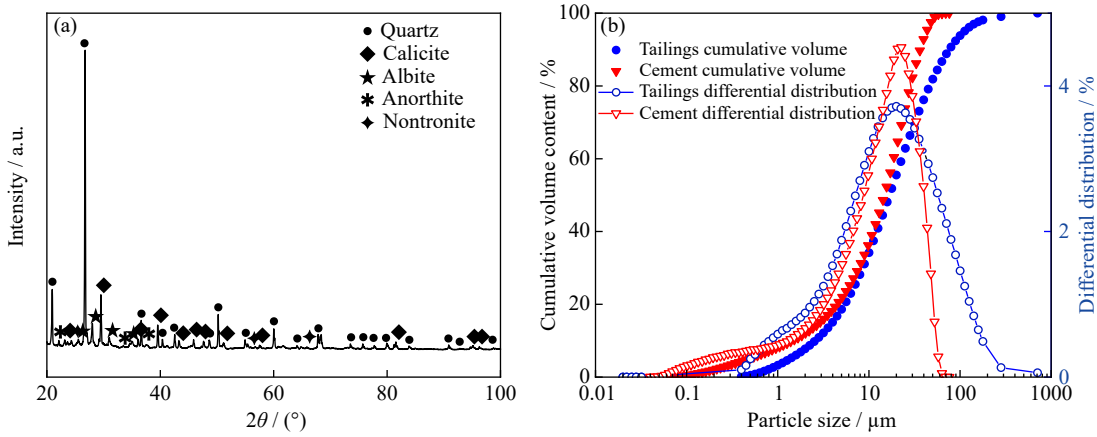

Fig. 1. (a) XRD patterns of tailings; (b) particle size distribution of experimental materials.

Table 1. Main chemical components of tailings wt%

Pb	S	As	Cu	Ag	CaO	MgO	Al_2O_3	SiO_2	Others
0.7	0.39	0.057	0.05	1.59	9.26	1.4	6.19	64.68	15.83

cement (32.5), and the particle size distribution is shown in Fig. 1, with an average particle size of 37 μm. According to the test, its chemical composition is detailed in Table 2, with the specific surface area of 4.1 $m^2 \cdot kg^{-1}$ and a specific gravity of 3.15.

Table 2. Main chemical components of cement wt%

MgO	SiO_2	Na_2O	K_2O	Al_2O_3	SO_3	Fe_2O_3	CaO	Others
1.40	20.70	0.18	0.48	4.50	2.60	3.30	65.10	1.74

In order to analyze the effect of admixture on the interaction force between particles, a super-plasticizer (naphthalene-based) produced by BASF [25] was selected as the admixture, which was commonly used to reduce the yield stress of slurry, thus reducing the pipeline transit resistance.

2.2. Experimental instruments

The FBRM was adopted to quantify the particle population characteristics (particle number and chord length) in order to analyze the particle dynamics evolution in the slurry. The whole experimental setup included FBRM probe, a beaker containing samples, a computer, and test bench, with installing the FBRM probe at an angle of 45° to detect a larger spatial range, fixing the beaker on the test bench, and rotating it at a speed of 10 r/min along with the bench. During the test, the computer recorded the data every 10 s, and each group of experiments was tested for 30 min. The FBRM allows *in-situ* acquisition of characteristic parameters of the sample particle population with a fine probe (9.5 mm) and minimal interference with the experiment without sample collection or dilution. Based on the FBRM technology, this investigation examined the particle population characteristics of the paste slurry, including particle number and chord length distribution. The chord length is the straight-line distance from one end of a particle to the other, and in particles that resemble spheres, it can be approximately equal to the diameter. The values in different directions were obtained through from multiple channels and the weighted average was obtained as the final value to reduce the errors. Its mathematical significance is shown in Eq. (1) below.

$$\overline{C} = \frac{\sum_{i=1}^{K}\left[\left(\frac{n_i}{\sum_{i=1}^{K} n_i}\right) M_i\right]}{\sum_{i=1}^{K}\left(\frac{n_i}{\sum_{i=1}^{K} n_i}\right)} = \frac{\sum_{i=1}^{K} n_i M_i}{\sum_{i=1}^{K} n_i} \tag{1}$$

where $\overline{C}$ is the chord length, n_i is the unweighted statistics, M_i is the midpoint value of the channel, and K is the channel numbers.

During the operation of the instrument, the aggregated laser beam passed through the internal lens of the probe, and was refocused near the instrument window as well as scanned at high rotational speed at the same time. As particles and particle aggregates appeared in the scanning path of the laser, the probe detected the light source reflected back from the surface of the particles and particle aggregates. At a constant beam scanning speed, the duration of the reflected pulse is proportional to the particle's width, which indicates that we can obtain the chord length distribution of particles or flocs and count fundamental parameters such as the number of particles with different lengths. The experimental set-up is shown in Fig. 2.

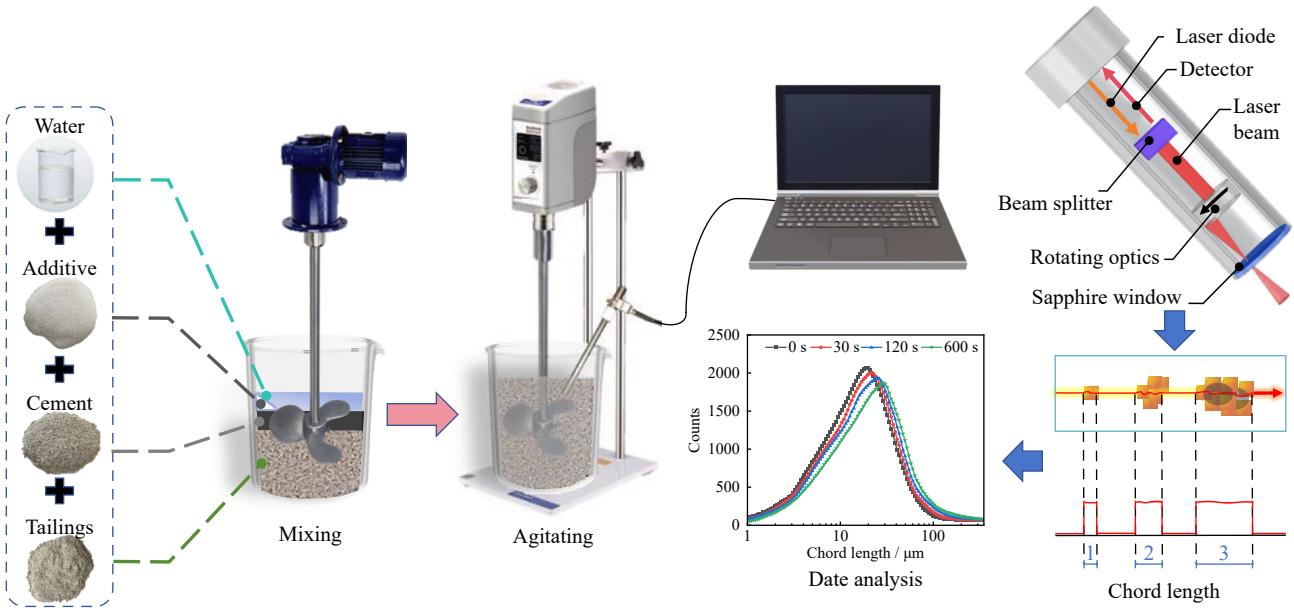

Fig. 2. Schematic diagram of experimental equipment and principles.

2.3. Experimental process

Sample preparations: First, adding the tailing sand and cement into a 2 L bucket and pre-mixing manually for 1 min; then, adding a predetermined amount of deionized water and mixing manually again for 1 min to obtain a relatively homogeneous mixture; subsequently, a handheld experimental stirrer was used to stir at 75 r/min for 5 min until the paste was homogeneous; finally, transfering the paste samples swiftly to the FBRM experimental beaker and starting the FBRM ex-

periment immediately. The basic flow is shown in Fig. 2.

The paste ratios are displayed in Table 3. Eight experimental groups were set with three different mass contents (68wt%, 70wt%, and 72wt%), two different cement–sand ratios (1:6 and 1:8), and the 1wt% admixture (P-4). Furthermore, the P-6, P-7, and P-8 groups were subjected to an additional continuous disturbance during the test, which was used to analyze the particle kinetic characteristics under various stirring rates (denoted by N).

Rheological testing is one of the most direct methods for understanding the rheological characteristics of paste [26]. The experimental process was repeated for the experimental groups, and fresh slurries were taken out for rheological tests. The instrument was a BROOKFIELDR/S plus rheometer equipped with a v40-20 paddle rotor (with a paddle diameter D of 20 mm and height H of 40 mm). The test was carried out in controlled shear rate mode (CSR) [27], and the obtained data was fitted by the Bingham model [28].

Table 3. Experimental proportion and condition change

Group	Solids content / wt%	Cement–sand ratio	Admixture / wt%	Mixing speed / (r·min^{-1})	Stirring rate / (r·min^{-1})
P-1	68	1:6	0	75	0
P-2	70	1:6	0	75	0
P-3	72	1:6	0	75	0
P-4	70	1:6	1	75	0
P-5	70	1:8	0	75	0
P-6	70	1:6	0	75	50
P-7	70	1:6	0	75	75
P-8	70	1:6	0	75	100

3. Results and discussion

3.1. Experimental results and analysis

The FBRM probe was utilized to make real-time, *in-situ* observations of the structural changes in the paste slurry to obtain the characteristics of the particle population at different moments, and plot the relationship between time and particle number, as shown in Fig. 3. Fig. 3(a) and (b) depicts the effects of the slurry ratio and stirring rate on the experimental results, respectively. The variations in the curves indicate that the evolutions of the particle population characteristics have been through two distinct stages, the dynamic phase and the stable phase. In the dynamic phase, the number of particles fluctuates with time, whereas in the stable phase, the number of particles remains in basic equilibrium. Moreover, by comparison, it can be observed that in Fig. 3(a), the particles of the paste slurry in their stationary condition adsorb to one another, tend to aggregate and decrease in number. As the rate of external shear stirring rises, the tendency of flocs to rupture increases.

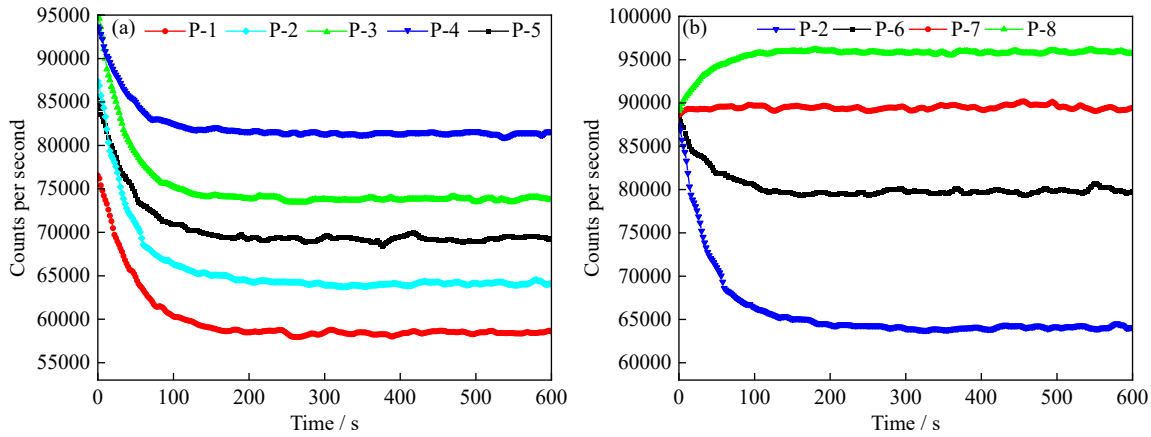

Fig. 3. Counts per second when subjected to different conditions: (a) different slurry ratios; (b) different stirring rates.

In order to more intuitively feedback the kinetic changes of particle and floc chord lengths at different moments, the chord length distribution characteristics of P-2 and P-8 are retrieved at 0, 20, 100, and 600 s, and the distribution curves are plotted in Fig. 4. The chord lengths at different moments are nearly normally distributed, with the peaks of the curves all around 20 μm. Fig. 4(a) shows the chord length distribution of the flocs of P-2 sample under stationary conditions. It can be seen that the peak point of the curve moves to the right, while the peak gradually decreases, which indicates that the particle aggregation occurs as the small particles gradually turn into large flocs. Nevertheless, Fig. 4(b) shows the chord length distribution of P-8 slurry under shear disturbance, from which the peak point of the curve moves to the left and the peak gradually increases. It suggests that the flocs decompose under shear disturbance, the small flocs increase, and the large flocs decrease.

In addition, Fig. 5 illustrates the difference in chord length percentage between the two experimental slurry groups with 0 and 100 r/min stirring rates at various times. A positive

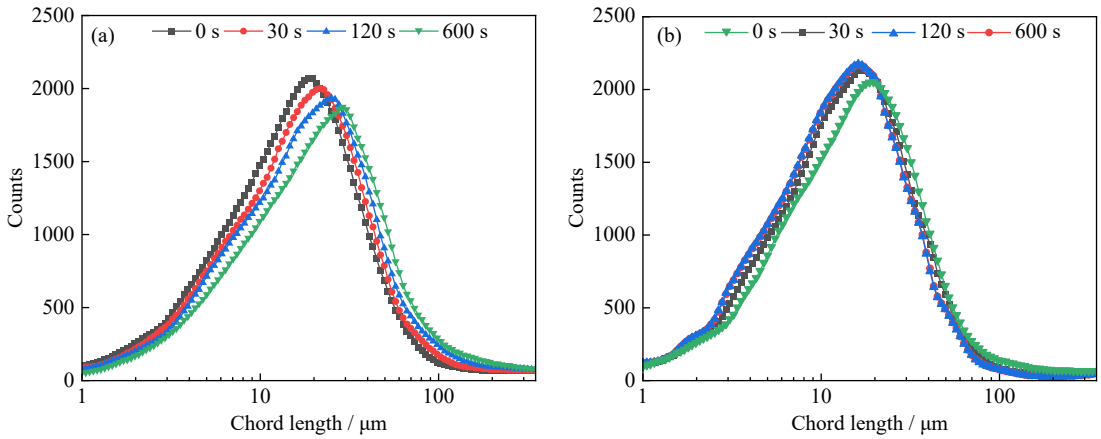

Fig. 4. Mean chord length evolution when subjected to different agitating conditions: (a) $N = 0$; (b) $N = 100$ r/min.

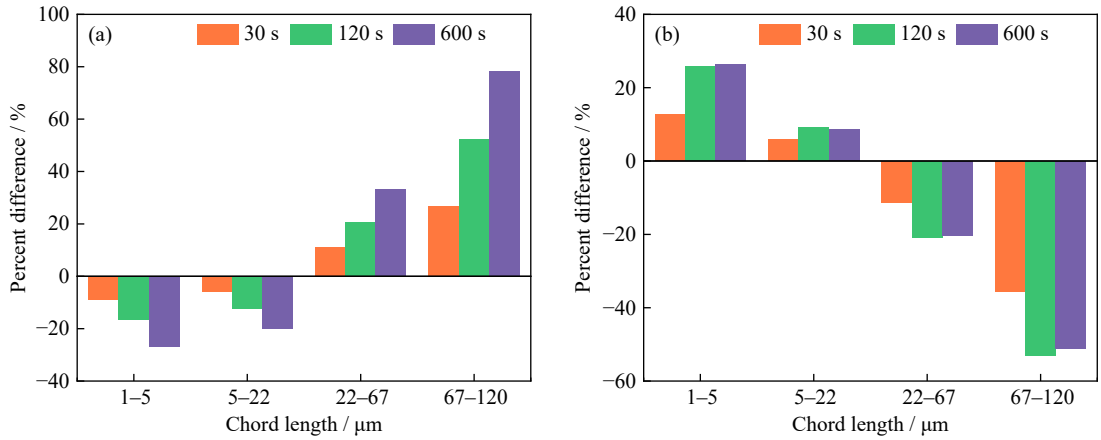

Fig. 5. Percentage difference of average chord length at different times: (a) $N = 0$; (b) $N = 100$ r/min.

number denotes an increase in particles, and a negative number suggests a decrease. It can be seen that the aggregation kinetics dominates the paste slurry at rest with the percentage of small flocs decreasing and the percentage of large flocs increasing, while the aggregation dynamics dominates under shear stirring with the percentage of small flocs increasing and the percentage of large flocs decreasing. Comparing Figs. 3–5, it can be found that the chord length distribution of flocs at rest varies continuously until 225 s, showing that the flocs are becoming longer in aggregate, while the chord length distribution of flocs at 100 r/min shear stirring is almost steady after 90 s, which demonstrates that the flocs are decomposing and reorganizing rapidly.

3.2. Particle aggregation and breakage kinetics

Unstable suspended particle aggregation process is called the flocculation phenomenon, which consists of two steps: aggregation and breakage. However, in fact, the current research on the evolution of suspended particles is insufficient due to the complexity of theoretical studies and the neglect for aggregate/floc/agglomerate breakage. Smoluchowski proposed the core theory that laid the foundation for all subsequent flocculation modeling studies, which is colloidal fast coalescence theory [23]. The theory aims to study the kinetics of particle aggregation and floc breakage processes and establish the Smol equation based on the evolution of the particle number concentration.

$$\frac{\mathrm{d}n_d}{\mathrm{d}t} = \frac{1}{2}\sum\nolimits_{a+j=d}\beta(a,j)n_a n_j - \sum\nolimits_{a=1}^{\infty}\beta(a,d)n_a n_d \tag{2}$$

where a, j, d is particle size, n_a and n_j is the particle concentration of a and j, t is time, and $\beta(a, j)$ is the collision frequency between particles of size a and j.

As the research on the rheology of suspended materials evolved, it was found that the particle kinetic evolution process was not restricted to Smol's three assumptions. All particle collisions lead to adhesion, all particles are spherical in shape, and collisions occur only between two particles. Based on the Smol equation, Thomas combined with Levich's theory of splitting incompatible solutions argued that flocs distort and finally break up due to enormous pressure variations on opposing sides. Based on this, the Thomas model [29] was proposed. Floc rupture is balanced by small particle collisions and aggregation, and the theory relates particle aggregation–breakage under shear to measurable parameters of:

$$\frac{\mathrm{d}N_\mathrm{A}}{\mathrm{d}t} = \delta N_\mathrm{B} - kN_\mathrm{A}^2 \tag{3}$$

where δ is the rate constant of floc deformation and rupture; t is time; k is the rate constant; N_A is the floc concentration of type A (produced by B-type deformation and rupture); N_B is a type B (larger size) floc concentration.

Generally, the Thomas model calculation needs to be based on the premise of clarifying the concentrations of large and small flocs. However, the flocs are rapidly dispersed and polymerized under the shearing action, and the large as well

as small flocs are converted to each other, which cannot accurately define the amount variations of the flocs, thus resulting in obvious deviations in the calculation results [30]. In order to better explain the paste kinetic evolution process, the paste particle kinetic constants k_1 and k_2 were proposed to study the flocculation and breakage process from the kinetic point of view by citing the research results in the field of cement paste [31]. There is a certain difference in the particle size distribution (PSD) of tailings and cement. There are more particles larger than 76 μm in tailings (9.3%) than those in cement (0.6%), and the quantity of particles smaller than 5 μm in cement (21.3%) is more than that in tailings (19.6%). The kinetic model primarily describes the aggregation and decomposition process of particles and flocs. Although different types and properties of particles exert a certain degree of influence on this process, this influence is primarily reflected in the variations of the particle kinetic constants k_1 and k_2. The differences between cement and tailings particles in terms of the particles align with the normal application of the kinetic model. Therefore, the paste slurry (tailings particles or cement particles) is considered as a composite system for research [32]. Based on the evolution law of particle number concentration, the kinetic properties of flocculation, breakage, and re-flocculation processes are studied, and the following differential equation is proposed:

$$\frac{\mathrm{d}n}{\mathrm{d}t} = -k_1 n^2 + k_2 n \tag{4}$$

where n is the number of particles, t is the time (in s), k_1 is the particle aggregation constant, and k_2 is the particle disaggregation constant.

Under experimental conditions, it can be assumed that the final microstructure of the paste is stable at a specific shear rate and the number of particles and flocs remains in dynamic equilibrium ($\frac{\mathrm{d}n}{\mathrm{d}t} = 0$), i.e.:

$$n = \frac{k_2}{k_1} \tag{5}$$

The model assumes that flocculation occurs in the collision of two particles and the breakage is the result of pressure fluctuations on both sides of the aggregate relative to each other, creating expansion deformation and eventual rupture. The experimental evolution of the flocs is fitted using the solved differential equation to obtain the theoretical model:

$$n_t = \frac{\frac{k_2}{k_1}}{1 - \left(\frac{n_0 - \frac{k_2}{k_1}}{n_0}\right) \mathrm{e}^{-k_2 t}} \tag{6}$$

where n_t is the number of particles at time t, n_0 is the initial number of particles.

3.3. Influencing factors of particle dynamics

Flocculation and breakage are mutually reversible phenomena [33] affected by the synergistic effect of internal and external factors of the slurry. The kinetic model constructed (Eq. (6)) was fitted to the experimental data to analyze the effect of various factors within on the kinetics of the paste particles.

3.3.1. Influences of content, cement–sand ratio, and admixture

The floc structure with certain strength is formed after particle collision and adsorption, and its structural strength is closely related to the number of particles, the nature of the tailing sand, the type of flocculant, and the size of the structure [34]. In order to analyze the law of particle kinetic evolution influenced by its internal factors, the experimental results of the paste with different contents, different cement–sand ratios, and added admixtures were fitted and analyzed. The average value was taken as the number of particles in the stabilization stage, and the results are shown in Table 4.

Table 4 displays the changes in the kinetics of the paste particles for varied contents of P-1 (68%), P-2 (70%), and P-3 (72%), with a goodness-of-fit coefficient R^2 greater than 0.94 for the tested samples, indicating a relatively excellent fit of the theoretical model. The comparison among P-1, P-2, and P-3 reveals that the number of particles per unit volume (n_0) grows with the content. The higher the mass content, the more solid particles content per unit volume. Also, the aggregation kinetics (k_1) of the paste appears to rise with increasing content, as does the rate of change in particle number, as shown in Fig. 6. This is due to the increased particle density increasing the encounter chance between particles and flocs as well as the mutual aggregation chance, resulting in an increase in the rate of anisotropic flocculation and isotropic flocculation, which makes it easy to form more stable flocs. However, contrary to the usual understanding, the slurry decomposition constant also increases (0.0191 → 0.0251) when the solid content increases (68% → 72%). This phenomenon may be related to the collisional decomposition of flocs. The increase in solid content increases the likelihood that flocs will collide with other particles or flocs. The possible mutual aggregation of particles or flocs as a result of collisions can also lead to the decomposition of colliding flocs, which makes the breakage constant increase signific-

Table 4. Kinetics constants of CPB groups P-1–P-5

Group	k_1 / 10^{-7}	k_2	n_0	$n_\infty = \frac{k_2}{k_1}$		R^2
				Theoretical quantity	Measured quantity	
P-1	3.27	0.0191	77579	58409.79	58447	0.973
P-2	3.35	0.0215	88978	64179.10	64055	0.947
P-3	3.40	0.0251	96419	73823.53	73818	0.942
P-4	3.13	0.0255	94246	81469.65	81414	0.946
P-5	3.15	0.0218	86154	69206.35	69265	0.968

antly. Based on the above analysis, it can be concluded that the paste content increases its stability and the resistance to stirring and dissociation increases. Hence, increasing the paste content during deep backfill not only reduces the conveying flow rate, but also helps the slurry maintain good performance under shock vibration.

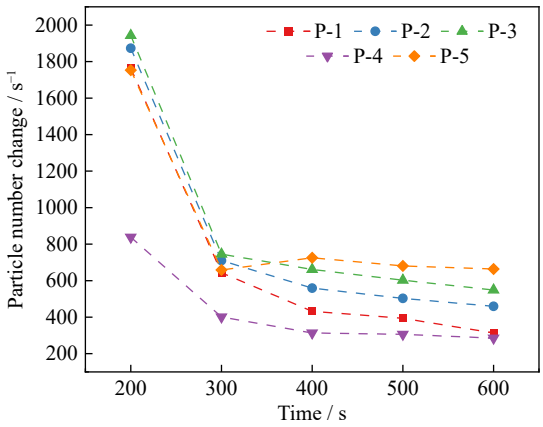

Fig. 6. Change of particle number under different conditions.

Besides, adding admixtures also plays a significant role in the evolution of slurry particle size. It is generally acknowledged that the plasticizer enhances the paste fluidity by reducing the particle interaction force and spatial site resistance effect to make the particles homogeneous and dispersed. As can be seen from Table 4, the aggregation constant k_1 with the addition of 1wt% content of admixture paste (P-4) is significantly reduced compared to that without admixtures (P-2), while the breakage constant k_2 is significantly increased, and the initial (n_0) and the average number of particles at dynamic equilibrium (n_∞) are also significantly increased. On the one hand, this is because the spatial site resistance of the plasticizer molecules affects the particle aggregation and flocculation, resulting in a substantial decrease in the slurry aggregation kinetic constant. On the other hand, the formed flocs are looser internally due to the adsorption of the admixture on the particle surface, while the plasticizer increases the repulsive force between the solid particles and the flocs are more likely to be broke up and dispersed, thus the measured slurry breakage kinetics increase. As shown in Fig. 6, the addition of the admixture significantly reduces the rate of particle change. Since the flocs are affected by breakage kinetics, interparticle aggregation is reduced and the quantities remain in dynamic equilibrium.

Moreover, the cement–sand ratio also has a significant effect on the particle dynamics of the CPB. As can be seen from Table 4, when the cement–sand ratio is reduced from 1:6 to 1:8, the paste aggregation constant k_1 decreases, while the breakage kinetic constant k_2 increases, and the number of particles and flocs contained in the paste slurry increase significantly. It indicates that increasing the cement addition enhances the interparticle forces, while the floc structure formed by the particles is more stable due to more early hydration products and stronger interparticle friction and cohesion. While the interparticle adsorption force is smaller for low cement–sand ratio, the stability of floc structure decreases, and the floc fragmentation and decomposition in the slurry is more frequent.

3.3.2. Shear stirring

During the backfill and conveying process, the paste is subjected to shear, shock, and vibration on the pipe wall, particularly in deep backfill and conveying. Therefore, it's of great necessity to investigate the effect of shear stirring on particle dynamics. The prepared fresh paste was simulated by controlling the disturbance rate (0, 50, 75, and 100 r/min) for the conveying process and monitoring the changes of its internal particle population characteristics. The results are shown in Table 5.

Table 5. Kinetics constants of P-2, P-6, P-7, and P-8

Group	k_1 / 10^{-7}	k_2	n_0	$n_\infty = \frac{k_2}{k_1}$		R^2
				Theoretical quantity	Measured quantity	
P-2	3.35	0.0215	88978	64179.10	64055	0.947
P-6	3.34	0.0267	88352	79940.12	79785	0.953
P-7	3.35	0.0302	89011	89552.24	89510	0.941
P-8	3.35	0.0323	89051	96130.95	95937	0.955

As can be seen, the parameters of the breakage constant (k_2) and the number of particles at stable equilibrium (n_∞) show an upward trend under different stirring states, while the aggregation constant (k_1) does not change significantly. k_2 increases from 0.0215 to 0.0323, increasing by about 50.2%, which is nearly 5 orders of magnitude higher than k_1, and n_∞ increases by 34.4%. As seen in Figs. 4 and 5, when the stirring speed increases from 0 to 100 r/min, the average chord length of particles within the slurry drops from 24.8 to 23.3 μm. It indicates that the breakage kinetics in the slurry gradually dominates as the disturbance rate increases, making the flocs tend to be dispersed and the number of particles increases while the average chord length decreases. Based on the results in Table 5, the relationship between shear disturbance and decomposition constants is plotted in Fig. 7. Besides, Fig. 8 shows the change law of percentage difference of flocs greater than 65 μm from beginning to end.

In order to better understand their mathematical relationship, Origin software was used to fit and analyze the data, and the results are shown as follows:

$$k_2 = 1.1 \times 10^{-4} N + 0.02147 \quad (7)$$

where k_2 is the particle breakage constant and N is the stirring rate.

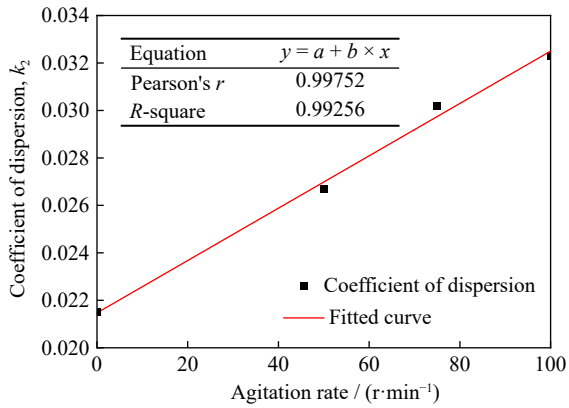

Fig. 7. Relationship between agitation rate and coefficient of breakage.

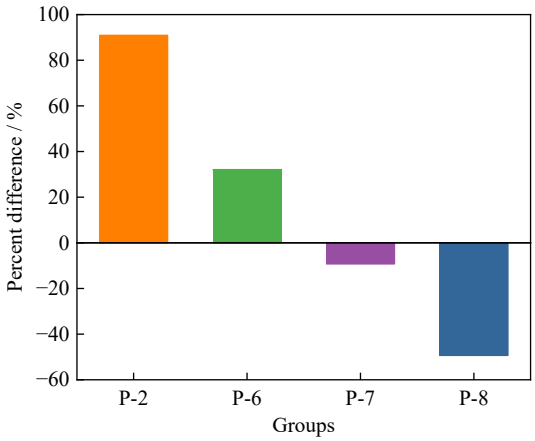

Fig. 8. Percentage difference of flocs greater than 65 μm from beginning to end.

Fig. 7 demonstrates that the stirring rate is positively correlated with the particle breakage kinetics. Combined with Fig. 5 and Fig. 8, it can be concluded that the larger flocs are sheared and decomposed into smaller flocs under high shear, and the number of flocs with larger chord lengths in the slurry is significantly reduced. When there is no stirring (P-2), the aggregation kinetics in the slurry dominates, and the fine particles (or flocs) gradually decrease, while the large flocs gradually increase and finally reach equilibrium. This indicates that the slurry is disturbed by external shear and breaks the original relatively stable floc structure, thus the relatively large particles lose the suspension of fine particles, which makes the slurry easier to be segregated and cause the pipe plugging accidents. During deep backfill, the shock vibrations of the slurry are amplified. As a result, understanding and accurately managing dynamics of paste are critical to the steady-state transport of CPB. For example, the addition of thickeners and nanoclays to CPB can enhance the aggregation kinetics of the paste, thus maintaining stability during transportation.

3.3.3. Rheological behavior

In order to understand the influence of particle kinetics on the rheological performance of paste, groups P-2, P-5, P-6, P-7, and P-8 were selected to conduct the research on the rheological performance of paste. Among them, groups P-2 and P-5 were adopted to investigate the influence of aggregation kinetics on rheological performance since the breakage kinetics of paste were basically the same. The aggregation kinetics of paste slurry in P-2 and P-6, 7, and 8 groups remained basically unchanged. Therefore, they were used to investigate the influence of breakage kinetics on rheological performance, and the relevant parameters were fitted according to the rheological test results as shown in Fig. 9.

Remarkably, there is a correlation between the rheological performance of the paste slurry and the particle kinetics. Rheological performance tests on the paste slurry with different cement–sand ratio show that with the increase of the cement–sand ratio, the aggregation kinetics (k_1) of the paste slurry increase. Besides, the yield stress of the paste slurry increases from 193.855 to 206.316 Pa, and the plastic viscosity increases from 0.2835 to 0.3127 Pa·s. This shows that the increase of aggregation kinetics are capable to lead to poor slurry liquidity when the breakage kinetics are stable. Combined with the FBRM test results, the comparative analysis of P-2 and P-5 groups shows that an increasing in aggregation kinetics means a dominated role of aggregation kinetics, thus the flocculation of particles are facilitated and the frictional force between particles is increased. In addition, the relative movement between particles is weakened. Therefore, the liquidity of paste slurry decreases. This phenomenon indicates that the deterioration of the macro-liquidity of the paste slurry

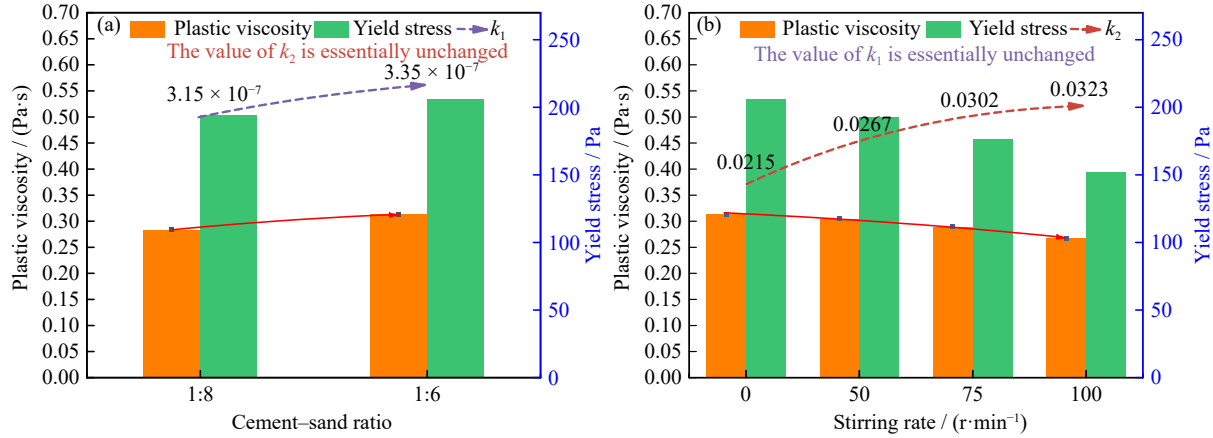

Fig. 9. Relationship between rheological parameters and particle dynamics: (a) different cement–sand ratio; (b) different stirring rate.

is caused by the change of its microstructure, which is consistent with the change law of particle number in Fig. 6.

Rheological performance test on paste slurry at different disturbance rates shows that when the disturbance rate is increased from 0 to 100 r/min, the breakage kinetics (k_2) of the paste slurry are increased. Besides, the yield stress of the paste slurry is decreased from 206.316 to 151.118 Pa, and the plastic viscosity is decreased from 0.3127 to 0.2894 Pa·s. This phenomenon shows that after the paste slurry is subjected to high shearing action, the yield stress and plastic viscosity are significantly reduced, demonstrating the thixotropy of shear thinning. Combined with Fig. 9(b), it can be seen that the particles adsorb each other to form a stable aggregate and mesh structure in the state of no disturbance. Correspondingly, the yield stress and plastic viscosity of the paste slurry are higher. With the increase of shearing rate, the breakage kinetics dominates, thus the aggregate particles and mesh structure inside the slurry being destroyed. The larger flocs are decomposed into smaller flocs, and the yield stress and plastic viscosity of the paste slurry are gradually reduced. In summary, the macroscopic of the paste slurry is affected by the microstructure, and the change of the microstructure is controlled by particle kinetics. The research findings are of great significance for the regulation of paste rheological behavior.

In summary, the particle evolution within the paste is regulated by the coordinated effects of internal (content, cement–sand ratio, admixture) and external factors (shear stirring). Based on the previous research results, the influence of internal factors of the slurry on particle dynamics is unified from the theoretical model, and the complex influence mechanism is summarized into aggregation constant and breakage constant, which is of great theoretical significance for understanding the complex rheological behavior of CPB from the perspective of mesostructure.

4. Conclusions

(1) The particle dynamics in the paste is influenced by the synergistic effect of internal and external factors, and the evolution process is roughly divided into dynamic and stable phases. In the dynamic stage, the particle evolution law is controlled by the kinetic constants k_1 and k_2. As the aggregation kinetics dominates, the fine particles aggregate into large flocs, the number of particles decreases, and the average chord length increases. When the breakage kinetics dominates, the large flocs decompose into fine particles, the number of particles increases, and the average chord length decreases. The time required for floc aggregation (225 s) is much longer than that for decomposition (90 s), and the disaggregation constant of the paste slurry is nearly five orders of magnitude higher than the aggregation constant. Still, breakage under shear occurs more quickly, as evidenced by the longer time required for aggregation than for breakage.

(2) The particle dynamics is influenced by factors such as paste content, admixture, and cement–sand ratio. As the content increases, the number of particles per unit volume increases, and the aggregation kinetics and breakage kinetics are enhanced. The admixture reduces the particle interaction force and its spatial site resistance effect, which makes the aggregation kinetics decrease and the breakage kinetics increase. Increasing the paste to gray sand ratio, the inter-particle friction and cohesion increases, the aggregation kinetics is enhanced, and the fine structure of the slurry is more stable.

(3) The flocculation process of paste is the equilibrium process of continuous aggregation of particles and breakage of flocs, which is more sensitive to the influence of external stirring. The disaggregation constant is positively correlated with the stirring rate. As the external stirring applied to the paste increases, its breakage kinetics constant is enhanced, and the inter-particle flocculent mesh structure is broken owing to the fragmentations of large flocs into smaller flocs or particles. The rheological results show that particle kinetics influence the macroscopic rheological behavior of the paste.

Acknowledgements

This study was financially supported by the National Natural Science Foundation of China (No. 52104129), the Shandong Provincial Major Science and Technology Innovation Project, China (No. 2019SDZY05), the key Laboratory of Mine Ecological Effects and Systematic Restoration, Ministry of Natural Resources (No. MEER-2022-09), the Double First-class Construction Project in Henan Province, China (No. AQ20230735), and the Doctoral Fund of Henan Polytechnic University (No. B2021-59).

Conflict of Interest

Aixiang Wu is the editor-in-chief and Huazhe Jiao is an editorial board member for this journal. They were not involved in the editorial review or the decision to publish this article. The authors declare that they have no known competing financial interests or personal relationships that could have appeared to influence the work reported in this paper.

References

[1] A.X. Wu, Y. Wang, Z.E. Ruan, B.L. Xiao, J.D. Wang, and L.Q. Wang, Key theory and technology of cemented paste backfill for green mining of metal mines, *Green Smart Min. Eng.*, 1(2024), No. 1, p. 27.

[2] H.Z. Jiao, W.X. Zhang, Y.X. Yang, *et al*., Static mechanical characteristics and meso-damage evolution characteristics of layered backfill under the condition of inclined interface, *Constr. Build. Mater.*, 366(2023), art. No. 130113.

[3] J.Y. Wu, H.W. Jing, Y. Gao, Q.B. Meng, Q. Yin, and Y. Du, Effects of carbon nanotube dosage and aggregate size distribution on mechanical property and microstructure of cemented rockfill, *Cem. Concr. Compos.*, 127(2022), art. No. 104408.

[4] L.H. Yang, J.C. Li, H.B. Liu, *et al*., Systematic review of mixing technology for recycling waste tailings as cemented paste backfill in mines in China, *Int. J. Miner. Metall. Mater.*, 30(2023), No. 8, p. 1430.

[5] Q. Zhou, J.H. Liu, A.X. Wu, and H.J. Wang, Early-age strength property improvement and stability analysis of unclassified tailing paste backfill materials, *Int. J. Miner. Metall. Mater.*, 27(2020), No. 9, p. 1191.
[6] H.Z. Jiao, X. Chen, Y.X. Yang, X.M. Chen, L.H. Yang, and T.Y. Yang, Mechanical properties and meso-structure of concrete under the interaction between basalt fiber and polymer, *Constr. Build. Mater.*, 404(2023), art. No. 133223.
[7] F. Puertas, C. Varga, and M.M. Alonso, Rheology of alkali-activated slag pastes. Effect of the nature and concentration of the activating solution, *Cem. Concr. Compos.*, 53(2014), p. 279.
[8] H.Y. Cheng, S.C. Wu, X.Q. Zhang, and A.X. Wu, Effect of particle gradation characteristics on yield stress of cemented paste backfill, *Int. J. Miner. Metall. Mater.*, 27(2020), No. 1, p. 10.
[9] H. Temmen, H. Pleiner, M. Liu, and H.R. Brand, Convective nonlinearity in non-Newtonian fluids, *Phys. Rev. Lett.*, 84(2000), No. 15, p. 3228.
[10] H.Z. Jiao, S.F. Wang, Y.X. Yang, and X.M. Chen, Water recovery improvement by shearing of gravity-thickened tailings for cemented paste backfill, *J. Cleaner Prod.*, 245(2020), art. No. 118882.
[11] T. Belem and M. Benzaazoua, Design and application of underground mine paste backfill technology, *Geotech. Geol. Eng.*, 26(2008), No. 2, p. 147.
[12] S. Ouellet, B. Bussière, M. Aubertin, and M. Benzaazoua, Microstructural evolution of cemented paste backfill: Mercury intrusion porosimetry test results, *Cem. Concr. Res.*, 37(2007), No. 12, p. 1654.
[13] H. Zhang, S. Cao, and E. Yilmaz, Influence of 3D-printed polymer structures on dynamic splitting and crack propagation behavior of cementitious tailings backfill, *Constr. Build. Mater.*, 343(2022), art. No. 128137.
[14] A. Heath, P. Fawell, P. Bahri, and J. Swift, Estimating average particle size by focused beam reflectance measurement (FBRM), *Part. Part. Syst. Charact.*, 19(2002), No. 2, art. No. 84.
[15] H.J. Yim, J.H. Kim, and S.P. Shah, Cement particle flocculation and breakage monitoring under Couette flow, *Cem. Concr. Res.*, 53(2013), p. 36.
[16] H.Z. Jiao, W.B. Yang, Z.E. Ruan, J.X. Yu, J.H. Liu, and Y.X. Yang, Microscale mechanism of tailing thickening in metal mines, *Int. J. Miner. Metall. Mater.*, 30(2023), No. 8, p. 1538.
[17] Q.S. Chen, S.Y. Sun, Y.K. Liu, C.C. Qi, H.B. Zhou, and Q.L. Zhang, Immobilization and leaching characteristics of fluoride from phosphogypsum-based cemented paste backfill, *Int. J. Miner. Metall. Mater.*, 28(2021), No. 9, p. 1440.
[18] R.D. Ferron, S. Shah, E. Fuente, and C. Negro, Aggregation and breakage kinetics of fresh cement paste, *Cem. Concr. Res.*, 50(2013), p. 1.
[19] R.P. Ferron, *Formwork Pressure of Self-Consolidating Concrete*: *Influence of Flocculation Mechanisms*, *Structural Rebuilding*, *Thixotropy and Rheology* [Dissertation], Northwestern University, Evanston, 2008.
[20] E. Yilmaz, T. Belem, B. Bussière, M. Mbonimpa, and M. Benzaazoua, Curing time effect on consolidation behaviour of cemented paste backfill containing different cement types and contents, *Constr. Build. Mater.*, 75(2015), p. 99.
[21] B. Fitch, Current theory and thickener design, *Ind. Eng. Chem.*, 58(1966), No. 10, p. 18.
[22] D.N. Thomas, S.J. Judd, and N. Fawcett, Flocculation modelling: A review, *Water Res.*, 33(1999), No. 7, p. 1579.
[23] M.L. Xie and Q. He, Solution of Smoluchowski coagulation equation for Brownian motion with TEMOM, *Particuology*, 70(2022), p. 64.
[24] G.Z. Yin, X.F. Jing, Z.A. Wei, and X.S. Li, Study of model test of seepage characteristics and field measurement of coarse and fine tailings dam, *Chin. J. Rock Mech. Eng.*, 29(2010), Suppl. 2, p. 3710.
[25] D.W. Zhang, X.M. Sun, Z.Y. Xu, C.L. Xia, and H. Li, Stability of superplasticizer on NaOH activators and influence on the rheology of alkali-activated fly ash fresh pastes, *Constr. Build. Mater.*, 341(2022), art. No. 127864.
[26] H.Y. Cheng, Z.M. Liu, S.C. Wu, *et al*., Resistance characteristics of paste pipeline flow in a pulse-pumping environment, *Int. J. Miner. Metall. Mater.*, 30(2023), No. 8, p. 1596.
[27] S.H. Yin, J.M. Liu, W. Chen, Y.J. Shao, L.B. Wu, and X.T. Wang, Rheological properties of coarse aggregate at low temperature and its regression models, *J. Cent. South Univ. Sci. Technol.*, 51(2020), No. 12, p. 3379.
[28] A.X. Wu, Z.E. Ruan, and J.D. Wang, Rheological behavior of paste in metal mines, *Int. J. Miner. Metall. Mater.*, 29(2022), No. 4, p. 717.
[29] L.A. Glasgow and R.H. Luecke, Mechanisms of deaggregation for clay–polymer flocs in turbulent systems, *Ind. Eng. Chem. Fund.*, 19(1980), No. 2, p. 148.
[30] B.H. Cho, W. Chung, and B.H. Nam, Molecular dynamics simulation of calcium–silicate–hydrate for nano-engineered cement composites—A review, *Nanomaterials*, 10(2020), No. 11, art. No. 2158.
[31] C. Negro, A. Blanco, E. Fuente, L.M. Sánchez, and J. Tijero, Influence of flocculant molecular weight and anionic charge on flocculation behaviour and on the manufacture of fibre cement composites by the Hatschek process, *Cem. Concr. Res.*, 35(2005), No. 11, p. 2095.
[32] S.B. Grant, J.H. Kim, and C. Poor, Kinetic theories for the coagulation and sedimentation of particles, *J. Colloid Interface Sci.*, 238(2001), No. 2, p. 238.
[33] P. Jarvis, B. Jefferson, J. Gregory, and S.A. Parsons, A review of floc strength and breakage, *Water Res.*, 39(2005), No. 14, p. 3121.
[34] J. Plank, E. Sakai, C.W. Miao, C. Yu, and J.X Hong, Chemical admixtures — Chemistry, applications and their impact on concrete microstructure and durability, *Cem. Concr. Res.*, 78(2015), p. 81.